Performance Analysis of Multi-antenna Hybrid Satellite-Terrestrial Relay Networks in the Presence of Interference

Kang An[1], Min Lin[2,3†], *Member, IEEE*, Tao Liang[4], Jun-Bo Wang[3] *Member, IEEE*, Jiangzhou Wang[5], *Senior Member, IEEE*, Yongming Huang[6], *Member, IEEE*, and A. Lee Swindlehurst[7], *Fellow, IEEE*

1. College of Communications Engineering, PLA University of Science and Technology, Nanjing 210007, China

2. PLA University of Science and Technology, Nanjing 210007, China

3. National Mobile Communications Research Laboratory, Southeast University, Nanjing 210096, China

4. Nanjing Telecommunication Technology Institute, Nanjing 210007, China

5. School of Engineering and Digital Arts, University of Kent, Canterbury, Kent, CT2, 7NZ, UK

6. School of Information Science and Engineering, Southeast University, Nanjing 210096, China

7. Center for Pervasive Communications and Computing, University of California, Irvine, CA 92697, USA

(Emails: ankang@nuaa.edu.cn, linmin63@163.com †, liangtao63@sina.com, jbwang@seu.edu.cn, j.z.wang@kent.ac.uk, huangym@seu.edu.cn, swindle@uci.edu)

Abstract

The integration of cooperative transmission into satellite networks is regarded as an effective strategy to increase the energy efficiency as well as the coverage of satellite communications. This paper investigates the performance of an amplify-and-forward (AF) hybrid satellite-terrestrial relay network (HSTRN), where the links of the two hops undergo Shadowed-Rician and Rayleigh fading distributions, respectively. By assuming that a single antenna relay is used to assist the signal transmission between the multi-antenna satellite and multi-antenna mobile terminal, and multiple interferers corrupt both the relay and destination, we first obtain the equivalent end-to-end signal-to-interference-plus-noise ratio (SINR) of the system. Then, an approximate yet very accurate closed-form expression for the ergodic capacity of the HSTRN is derived. The analytical lower bound expressions are also obtained to efficiently evaluate the outage probability (OP) and average symbol error rate (ASER) of the system. Furthermore, the asymptotic OP and ASER expressions are developed at high signal-to-noise ratio (SNR) to reveal the achievable diversity order and array gain of the considered HSTRN. Finally, simulation results are provided to demonstrate the validity of the analytical results, and show the impact of various parameters on the system performance.

Index Terms

Hybrid satellite-terrestrial network, amplify-and-forward relay, co-channel interference.

I. Introduction

The land mobile satellite (LMS) systems have been widely applied in scenarios, such as navigation, broadcasting, rescue, and disaster relief, due to its potential in providing wide coverage and achieving high data rate transmission. However, the obstacles and shadowing between the satellite and terrestrial user may result in the masking effect, which makes a line of sight (LOS) communication difficult to be maintained [1]. The relay transmission, in which the relay forwards the received signal from a source to a intended destination, has attracted a lot of attention in various wireless communication systems, since it can increase the reliability and throughput with a given power or bandwidth [2]. A novel network architecture, referred as the hybrid satellite terrestrial relay network (HSTRN), has been proposed to exploit both advantages to significantly enhance the system performance (e.g. [3]).

A. Background and Motivation

A lot of effort has been devoted to investigating the performance of HSTRNs by employing various relay protocols, such as amplify-and-forward (AF) and decode-and-forward (DF). By assuming maximal ratio combining (MRC) at the destination, the authors of [4] studied the average symbol error rate (ASER) of HSTRN with AF relaying protocol of a variable gain , and an extended work to the AF-based hybrid satellite-terrestrial free space optical (FSO) cooperative systems was given in [5], where the asymptotic ASER behaviors have also been investigated. In [6], the authors presented the exact outage probability (OP) expression of a HSTRN with best relay selection scheme operating in DF protocol. The authors of [7] have considered the applicability of multi-satellite multiple-input multiple-output (MIMO) to satellite communications by employing a dual-satellite 2×2 MIMO channels with each satellite equipped with a single antenna. Moreover, the OP performance comparison of HSTRNs with fixed relaying (FR) and selection relaying (SR) protocols was presented in [8]-[9].

The researches in [4]-[9] were mainly focused on the scenarios where all the nodes are equipped with a single antenna. However, since the multi-antenna technique exhibits a significant advantage in achieving high system capacity and energy efficiency [10]-[12], the case of satellite having multiple antennas has received significantly attention more recently. When channel state information (CSI) is available, a practical strategy among a variety of multi-antenna techniques is beamforming (BF) due to its low implementation complexity, which has been well studied in

[10]. The work [13] has analyzed the performance of multiple antenna satellite communication systems in one-hop scenarios, where the ergodic capacity, OP and ASER have been derived. The extended works of [13] to cases with estimation errors at the destination can be found in [14]. Since the relaying transmission has been proved as an effective approach to enhance the throughput and coverage of satellite communication, the authors of [15]-[20] have investigated the performance of relay-based multiple antenna HSTRNs with beamforming (BF). Specifically, in [15], the performance of multiple antenna HSTRN with both AF and DF protocols have been analyzed by deriving the exact closed-form expressions of OP and ASER. In [16], the performance of beamforming in AF-based HSTRNs with multiple antenna terrestrial relay and destination has been studied, where both the analytical and asymptotic ASER expressions have been derived. Moreover, [17] have investigated the DF-based satellite relaying with multi-antenna terrestrial source and destination, and an extended work to the AF-based scenarios can be found in [18]. By considering a two-way HSTRNs with multiple antennas at the relay, an approximate ASER expression based on moment generating function (MGF) was presented in [19]. The work [20] investigated the effect of antenna correlation on the performance of multiple antenna HSTRNs and gave the analytical expressions for OP, ASER, and ergodic capacity.

Although the aforementioned researches have significantly improved the performance and benefits of HSTRNs, they have assumed the ideal case of no co-channel interference (CCI), which is unrealistic in practical wireless systems. In recent years, a great deal of researches have focused on the performance of conventional terrestrial systems in the presence of CCI over Rayleigh or Nakagami-m fading channels [21]-[23]. Due to the reuse of spectrum resources in practice, the major challenges facing the hybrid satellite-terrestrial networks is the problem of interference from inter-component and/or intra-component [24]. While [25] has firstly investigated the ASER performance of the HSTRNs with CCIs at the destination for the single antenna scenario, the ergodic capacity, OP, and ASER have not been studied in the case that the satellite and terrestrial user have multi-antenna and CCIs corrupting both the relay and destination nodes. It is crucial to study this problem.

B. Contributions and Novelty

In this paper, we consider a multi-antenna AF HSTRN with multiple interferers at both terrestrial relay and destination, where the source-relay link undergoes Shadowed-Rician fading

while the relay-destination link experiences Rayleigh fading. By applying the maximal ratio transmission (MRT) at the source and maximal ratio combining (MRC) at the destination, the equivalent end-to-end output signal-to-interference-plus-noise ratio (SINR) of the system is first obtained, then analytical expressions as well as asymptotic results are derived to evaluate the system performance. The detailed contributions of this paper are outlined as follows:

- We present a new analytical expression for the ergodic capacity of the hybrid system, which is applicable for the cases of arbitrary number of interferers and antennas.
- The tight analytical expressions for the OP and ASER are derived, which can efficiently evaluate the system performance. This paper considers the multiple antenna scenarios with the presence of CCI, while [4]-[6] only considered single antenna scenario without the presence of CCI. Although [14] considered the multiple antenna case, it ignored the CCI in the system performance analysis.
- To gain further insight, the simple asymptotic expressions of OP and ASER at high SNR regime are developed to show the asymptotic behavior of the dual-hop AF relay network, in terms of two key parameters: diversity order and array gain.

Notations: $(\cdot)^H$ denotes the Hermitian transpose, $\|\cdot\|_F$ denotes the Frobenius norm of a matrix, $|\cdot|$ stands for the absolute value, $\mathrm{E}[\cdot]$ is the expectation, $\exp(\cdot)$ is the exponential function, and $\mathcal{N}_C(\mu, \mathbf{\Sigma})$ stands for the complex Gaussian distribution with mean μ and covariance matrix $\mathbf{\Sigma}$. ${}_1F_1(a; b; c)$ denotes the confluent Hypergeometric function [26, eq. (9.210.1)], $M_{a,b}(\cdot)$ is the Whittaker function [26, eq. (9.221)], $\mathrm{G}_{p,q}^{m,n}[\cdot|\cdot]$ is the Meijer-G functions with single variable [26, eq. (9.301)], $\mathrm{G}_{2,[2:1],1,[3:2]}^{2,1,1,3,2}[\cdot|\cdot]$ and $\mathrm{G}_{1,[1:1],0,[1:1]}^{1,1,1,1,1}[\cdot|\cdot]$ denote the Meijer-G functions of two variables [27].

II. System Model

Consider an AF HSTRN, where a geostationary satellite (S) communicates with a terrestrial destination (D) via a terrestrial relay (R). Here, the direct link between S and D is assumed to be unavailable due to heavy shadowing. Without loss of generality, the overall communication occurs during two time phases. During the first time phase, the satellite carries out transmit BF with weight vector $\mathbf{w}_1$ $(N_s \times 1)$ and sends the signal $x(t)$ to R through the fading channel $\mathbf{h}_1$ $(N_s \times 1)$. Meanwhile, R is corrupted by I_1 co-channel interferers $\{s_{1,i}(t)\}_{i=1}^{I_1}$ with an average power of $\{P_{1,i}\}_{i=1}^{I_1}$. As such, the received signal at the R can be written as

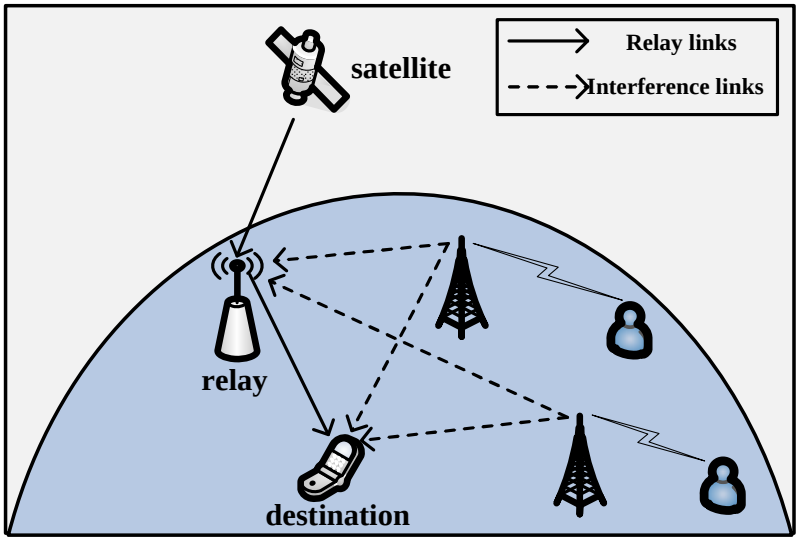

Fig. 1: System model of HSTRN with CCI at the relay and destination.

$$y_r(t) = \sqrt{P_s}\mathbf{w}_1^H \mathbf{h}_1 x(t) + \sum_{i=1}^{I_1} \sqrt{P_{1,i}} g_{1,i} s_{1,i}(t) + n_1(t), \tag{1}$$

where P_s denotes the transmit power at S, $x(t)$ is the transmit signal with $\mathrm{E}\left[|x(t)|^2\right] = 1$ and $n_1(t)$ is the zero mean additive white Gaussian noise (AWGN) at R satisfying $\mathrm{E}\left[|n_1(t)|^2\right] = \sigma_1^2$. In addition, $g_{1,i}$ is the channel coefficient for the i-th interference-relay link, which is subject to independently and identically distributed (i.i.d) complex Gaussian distribution.

During the second time phase, R first amplifies the received signal by a variable gain factor G as

$$G^2\left(P_s\left\|\mathbf{w}_1^H\mathbf{h}_1\right\|_F^2 + \sum_{i=1}^{I_1} P_{1,i}|g_{1,i}|^2 + \sigma_1^2\right) = 1, \tag{2}$$

and then sends it to D through the fading channel $\mathbf{h}_2\,(N_d \times 1)$. Under the condition that the destination is corrupted by I_2 interferers with the average powers of $\{P_{2,j}\}_{j=1}^{I_2}$, and received BF with weight vector $\mathbf{w}_2\,(N_d \times 1)$ is exploited, the output signal at D is given by

$$\mathrm{y}_d(t) = \mathbf{w}_2^H\left[\sqrt{P_r}G\mathbf{h}_2 y_r(t) + \sum_{j=1}^{I_2}\sqrt{P_{2,j}}\mathbf{g}_{2,j}s_{2,j}(t) + \mathbf{n_2}(t)\right], \tag{3}$$

where P_r is the transmit power at R, and $\mathbf{n_2}(t)$ the AWGN at D obeying $\mathbf{n}_2(t) \sim \mathcal{N}_C\left(\mathbf{0}, \sigma_2^2\mathbf{I}_{N_d}\right)$. $\{s_{2,j}(t)\}_{j=1}^{I_2}$ represents the interference signal with each obeying $\mathrm{E}\left[|s_{2,j}(t)|^2\right] = 1$, and $\mathbf{g}_{2,j}$ is the channel vector for the j-th interference-destination link satisfying $\mathbf{g}_{2,j} \sim \mathcal{N}_C\left(0, \mathbf{I}_{N_d}\right)$.

Assuming that perfect CSI is available at either S or D, MRT and MRC can be adopted[1], respectively, namely, $\mathbf{w}_1 = \mathbf{h}_1/\|\mathbf{h}_1\|_F$ and $\mathbf{w}_2 = \mathbf{h}_2/\|\mathbf{h}_2\|_F$. By using (1) and (2) for (3), after some algebraic manipulations, the output SINR at D can be expressed as

$$\gamma_d = \frac{\gamma_1\gamma_2}{\gamma_1\left(\gamma_3+1\right)+\gamma_2\left(\gamma_4+1\right)+\left(\gamma_3+1\right)\left(\gamma_4+1\right)} = \frac{\Gamma_1\Gamma_2}{\Gamma_1+\Gamma_2+1}, \tag{4}$$

where $\Gamma_1 = \gamma_1/(\gamma_3+1)$ with $\gamma_1 = P_s\left\|\mathbf{h}_1\right\|_F^2/\sigma_1^2 \triangleq \bar{\gamma}_1\left\|\mathbf{h}_1\right\|_F^2$ and $\gamma_3 = \sum_{i=1}^{I_1} P_{1,i}\left|g_{1,i}\right|^2/\sigma_1^2 \triangleq \sum_{i=1}^{I_1}\bar{\gamma}_{3,i}\left|g_{1,i}\right|^2$, $\Gamma_2 = \gamma_2/(\gamma_4+1)$ with $\gamma_2 = P_r\left\|\mathbf{h}_2\right\|_F^2/\sigma_2^2 \triangleq \bar{\gamma}_2\left\|\mathbf{h}_2\right\|_F^2$ and $\gamma_4 = \sum_{j=1}^{I_2} P_{2,j}\left\|\mathbf{w}_2^H\mathbf{g}_{2,j}\right\|_F^2/\sigma_2^2 \triangleq \sum_{j=1}^{I_2}\bar{\gamma}_{4,j}\left\|\mathbf{w}_2^H\mathbf{g}_{2,j}\right\|_F^2$. Here, $\bar{\gamma}_1$, $\bar{\gamma}_2$, $\bar{\gamma}_{3,i}$, and $\bar{\gamma}_{4,j}$ denote the average SNRs of each link.

In order to analyze the performance of a HSTRN, we first introduce some known results about the statistical properties of wireless fading channels, and then provide detailed derivation of the theoretical formulas of the ergodic capacity, OP, and ASER of the considered system.

III. Preliminary Results

Satellite-terrestrial links are usually modeled by composite fading distributions to describe more accurately the amplitude fluctuation of the signal envelope [18]. Although some mathematical models, such as Loo, Barts-Stutzman, and Karasawa *et al.*, have been presented to describe the satellite channel, the Shadowed-Rician model proposed in [28] is a popular one, which provides a significantly less computational burden than other channel models. The channel vector $\mathbf{h}_1$ with i.i.d Shadowed-Rician fading distribution is described as $\mathbf{h}_1 = \bar{\mathbf{h}}_1 + \tilde{\mathbf{h}}_1$, where the LOS component $\bar{\mathbf{h}}_1$ can be modeled as i.i.d Nakagami-m random variables and the entries of scattering component $\tilde{\mathbf{h}}_1$ follow the i.i.d Rayleigh fading distribution [28]. According to [29], by using the inverse Laplace transformation of the MGF, a well-approximated expression for the probability density function (PDF) and cumulative distributiuon function (CDF) of $\gamma_1 = \bar{\gamma}_1\left\|\mathbf{h}_1\right\|_F^2$ are, respectively, given by

$$f_{\gamma_1}(x) = \alpha^{N_s}\sum_{l=0}^{c}\binom{c}{l}\beta^{c-l}\left(\frac{x^{d-l-1}}{\bar{\gamma}_1^{d-l}\Gamma\left(d-l\right)}\,{}_1F_1\left(d;d-l;-\frac{\left(\beta-\delta\right)x}{\bar{\gamma}_1}\right)\right.$$

[1]In the presence of co-channel interference, the zero-forcing (ZF) or minimum mean-square error (MMSE) schemes may achieve a better performance. However, they require the CSI of the interfering links, which result in heavy implementation complexity. On the contrary, the MRC scheme adopted in this paper only requires the CSI of the satellite-relay link, which is easier to implement.

$$+\frac{\varepsilon\delta x^{d-l}}{\bar{\gamma}_1^{d-l+1}\Gamma\left(d-l+1\right)}{}_1F_1\left(d+1;d-l+1;-\frac{\left(\beta-\delta\right)x}{\bar{\gamma}_1}\right)\Bigg), \tag{5}$$

and

$$F_{\gamma_1}\left(x\right)=\alpha^{N_s}\sum_{l=0}^{c}\binom{c}{l}\beta^{c-l}\Bigg(\frac{\left(\beta-\delta\right)^{\frac{l-d-1}{2}}}{\bar{\gamma}_1^{\frac{d-l-1}{2}}\Gamma\left(d-l+1\right)}x^{\frac{d-l-1}{2}}e^{-\frac{\beta-\delta}{2\bar{\gamma}_1}x}M_{\frac{d+l-1}{2},\frac{d-l}{2}}\left(\frac{\beta-\delta}{\bar{\gamma}_1}xz\right)$$
$$+\frac{\varepsilon\delta(\beta-\delta)^{\frac{l-d}{2}}}{\bar{\gamma}_1^{\frac{d-l}{2}}\Gamma\left(d-l+2\right)}x^{\frac{d-l}{2}}e^{-\frac{\beta-\delta}{2\bar{\gamma}_1}x}M_{\frac{d+l}{2},\frac{d-l+1}{2}}\left(\frac{\beta-\delta}{\bar{\gamma}_1}xz\right)\Bigg), \tag{6}$$

where $\alpha=2bm/\left(2bm+\Omega\right)^m/2b$, $\beta=1/2b$, $\delta=\Omega/2b\left(2bm+\Omega\right)$ with Ω being the average power of LOS component, $2b$ is the average power of multipath component and m_i is the Nakagami-m parameter ranging from 0 to ∞, $c=(d-N_s)^+$, $\varepsilon=mN_s-d$, $d=\max\left\{N_s,\lfloor mN_s\rfloor\right\}$, where $\lfloor z\rfloor$ is the largest integer not greater than z, and $(z)^+$ indicates that if $z<0$, then let $z=0$.

Since R and D are two terrestrial nodes, the relay-destination link is often assumed to undergo Rayleigh or Nakagami-m fading distribution distribution [8], [16], [25]. Without loss of generality, we consider the terrestrial link $\mathbf{h}_2$ follows the Rayleigh fading and, the PDF and CDF of $\gamma_2=\bar{\gamma}_2\left\|\mathbf{h}_2\right\|_F^2$ are given by [21]

$$f_{\gamma_2}\left(x\right)=\frac{x^{N_d-1}}{(N_d-1)!\bar{\gamma}_2^{N_d}}e^{-\frac{x}{\bar{\gamma}_2}}, \tag{7}$$

and

$$F_{\gamma_2}\left(x\right)=1-e^{-\frac{x}{\bar{\gamma}_2}}\sum_{i=0}^{N_d-1}\frac{1}{i!}\left(\frac{x}{\bar{\gamma}_2}\right)^i. \tag{8}$$

Moreover, the PDF of $\gamma_3=\sum_{i=1}^{I_1}\bar{\gamma}_{3,i}\left|g_{1,i}\right|^2$ can be expressed as [21]

$$f_{\gamma_3}\left(x\right)=\sum_{i=1}^{I_1}\frac{\rho_i}{\bar{\gamma}_{3,i}}e^{-\frac{x}{\bar{\gamma}_{3,i}}}, \tag{9}$$

with the coefficients ρ_i being given by

$$\rho_i=\left[\prod\nolimits_{k=1,k\neq i}^{I_1}\frac{1}{(1+s\bar{\gamma}_{3,k})}\right]\Bigg|_{s=-\bar{\gamma}_{3,i}^{-1}}. \tag{10}$$

According to [23], since each entry of $\mathbf{g}_{2,j}$ is i.i.d complex Gaussian Random Variable (RV), by defining $f_j=\mathbf{w}_2^H\mathbf{g}_{2,j}$, it can be easily shown that $\left|f_j\right|^2$ follows the Rayleigh distribution. Thus, the PDF of $\gamma_4=\sum_{j=1}^{I_2}\bar{\gamma}_{4,j}\left\|\mathbf{w}_2^H\mathbf{g}_{2,j}\right\|_F^2=\sum_{j=1}^{I_2}\bar{\gamma}_{4,j}\left|f_j\right|^2$ can be written as

$$f_{\gamma_4}\left(x\right)=\sum_{j=1}^{I_2}\frac{\omega_j}{\bar{\gamma}_{4,j}}e^{-\frac{x}{\bar{\gamma}_{4,j}}}, \tag{11}$$

where the coefficients ω_j are given by

$$\omega_j = \left[\prod_{l=1,l\neq j}^{I_2} \frac{1}{(1+s\bar{\gamma}_{4,l})}\right]\Bigg|_{s=-\bar{\gamma}_{4j}^{-1}}. \tag{12}$$

IV. Performance Analysis

In this section, by using the method of Meijer-G functions, we derive analytical expression of the ergodic capacity, OP, and ASER of the considered HSTRN.

A. Ergodic Capacity

The average ergodic capacity is defined as the expected value of instantaneous mutual information of the end-to-end SINR, namely

$$C_{erg} = \frac{1}{2} E\left[\log_2\left(1+\gamma_d\right)\right], \tag{13}$$

where the coefficient 1/2 accounts for the fact that the entire communication occurs during two time phases. By substituting γ_d along with (4), (13) can be derived as

$$C_{erg} = \frac{1}{2} E\left[\log_2\left(\frac{\left(1+\Gamma_1\right)\left(1+\Gamma_2\right)}{\Gamma_1+\Gamma_2+1}\right)\right] = \frac{1}{2}\sum_{i=1}^{2} E\left[\log_2\left(1+\Gamma_i\right)\right] - \frac{1}{2} E\left[\log_2\left(1+\Gamma_3\right)\right] = \sum_{i=1}^{2} C_i - C_3, \tag{14}$$

where $\Gamma_3 = \Gamma_1 + \Gamma_2$, and $C_i = (1/2)\, E\left[\log_2\left(1+\Gamma_i\right)\right] (i = 1, 2, 3)$. The key procedure to obtain (14) is to find the first two terms $C_i\,(i=1,2)$ and the third term C_3, respectively.

For $i = 1, 2$, C_i can be expressed in terms of the PDF of Γ_i as

$$C_i = \frac{1}{2\ln 2}\int_0^\infty \ln\left(1+x\right) f_{\Gamma_i}\left(x\right) dx. \tag{15}$$

When the CCI dominates the noise, we can obtain the approximations $\Gamma_1 = \gamma_1/(\gamma_3+1) \approx \gamma_1/\gamma_3$ and $\Gamma_2 = \gamma_2/(\gamma_4+1) \approx \gamma_2/\gamma_4$ so that $f_{\Gamma_i}\left(x\right)(i=1,2)$ can be, respectively, approximated as

$$f_{\Gamma_1}\left(x\right) \approx \int_0^\infty z f_{\gamma_1}\left(xz\right) f_{\gamma_3}\left(z\right) dz, \tag{16}$$

$$f_{\Gamma_2}\left(x\right) \approx \int_0^\infty z f_{\gamma_2}\left(xz\right) f_{\gamma_4}\left(z\right) dz. \tag{17}$$

Theorem 1. *The closed-form expressions of C_1 and C_2 are given by (18) and (19), respectively.*

$$C_1 = \frac{\alpha^{N_s}}{2\ln 2}\sum_{l=0}^{c}\binom{c}{l}\beta^{c-l}\sum_{i=1}^{I_1}\rho_i\left(\frac{\bar{\gamma}_{3,i}^{d-l}}{\bar{\gamma}_1^{d-l}\Gamma\left(d\right)}\mathrm{G}_{4,4}^{3,3}\left[\frac{\left(\beta-\delta\right)\bar{\gamma}_{3,i}}{\bar{\gamma}_1}\middle|\begin{matrix}-d+l, 1-d, -d+l, 1-d+l\\ 0, -d+l, -d+l, 1-d+l\end{matrix}\right]\right.$$

$$+\frac{\varepsilon\delta\bar{\gamma}_{3,i}^{d-l+1}}{\bar{\gamma}_1^{d-l+1}\Gamma\left(d+1\right)}\mathrm{G}_{4,4}^{3,3}\left[\frac{\left(\beta-\delta\right)\bar{\gamma}_{3,i}}{\bar{\gamma}_1}\middle|\begin{matrix}-d+l-1,-d,-d+l-1,-d+l\\0,-d+l-1,-d+l-1,-d+l\end{matrix}\right]\Bigg), \tag{18}$$

$$C_2=\frac{1}{2\ln 2\left(N_d-1\right)!\bar{\gamma}_2^{N_d}}\sum_{j=1}^{I_2}\omega_j\bar{\gamma}_{4,j}^{N_d}\mathrm{G}_{3,3}^{3,2}\left[\frac{\bar{\gamma}_{4,j}}{\bar{\gamma}_2}\middle|\begin{matrix}-N_d,-N_d,-N_d+1\\0,-N_d,-N_d\end{matrix}\right], \tag{19}$$

where $\mathrm{G}_{p,q}^{m,n}\left[\cdot\,|\cdot\right]$ *is the Meijer-G functions with single variable.*

Proof. See Appendix A. □

Due to the fact that the closed-form PDF expression of $\Gamma_3=\Gamma_1+\Gamma_2$ is mathematically intractable, C_3 can not be calculated with the similar methods to C_1 and C_2. By using the definition of MGF, $M_{\Gamma_i}\left(s\right)\left(i=1,2\right)$ can be expressed with respect to the PDF of Γ_i as

$$M_{\Gamma_i}\left(s\right)=\mathrm{E}\left[e^{-s\Gamma_i}\right]=\int_0^\infty e^{-sx}f_{\Gamma_i}\left(x\right)dx. \tag{20}$$

Then, according to [30], C_3 in (14) is given by

$$C_3=\frac{1}{\ln 2}\int_0^\infty Ei\left(-s\right)M_{\Gamma_3}^{(1)}\left(s\right)ds, \tag{21}$$

where $Ei\left(-s\right)$ is the exponential integral function [26], $M_{\Gamma_3}^{(1)}\left(s\right)$ represents the first-order derivation of the MGF of Γ_3 with $M_{\Gamma_3}\left(s\right)=M_{\Gamma_1}\left(s\right)M_{\Gamma_2}\left(s\right)$. Furthermore, using Meijer-G functions, the analytical expression of (21) can be obtained through Theorem 2.

Theorem 2. *The closed-form expression of* C_3 *is given by (22) with* $I\left(\cdot,\cdot,\cdot,\cdot\right)$ *and* $J\left(\cdot,\cdot,\cdot,\cdot\right)$ *given by (23) and (24)*

$$C_3=\frac{\alpha^{N_s}}{2\ln 2}\sum_{l=0}^{c}\binom{c}{l}\beta^{c-l}\sum_{i=1}^{I_1}\rho_i\sum_{j=1}^{I_2}\frac{\omega_j\bar{\gamma}_{4,j}^{N_d}}{\left(N_d-1\right)!\bar{\gamma}_2^{N_d}}\Bigg(\frac{\bar{\gamma}_{3,i}^{d-l}}{\Gamma\left(d\right)\bar{\gamma}_1^{d-l}}\left[I\left(i,j,d,l\right)+J\left(i,j,d,l\right)\right]$$
$$+\frac{\varepsilon\delta\bar{\gamma}_{3,i}^{d-l+1}}{\Gamma\left(d+1\right)\bar{\gamma}_1^{d-l+1}}\left[I\left(i,j,d+1,l\right)+J\left(i,j,d+1,l\right)\right]\Bigg), \tag{22}$$

where

$$I\left(i,j,d,l\right)=\mathrm{G}_{2,[2:1],1,[3:2]}^{2,1,1,3,2}\left[\begin{matrix}\frac{\bar{\gamma}_1}{(\beta-\delta)\bar{\gamma}_{3,i}}\\\frac{\bar{\gamma}_2}{\bar{\gamma}_{4,j}}\end{matrix}\middle|\begin{matrix}-N_d-d+l,-N_d-d+l\\1,d-l,1\\-d+l-N_d\\1+d-l,1+d-l,d,N_d,N_d+1\end{matrix}\right], \tag{23}$$

$$J\left(i,j,d,l\right)=\mathrm{G}_{2,[2:1],1,[3:2]}^{2,1,1,3,2}\left[\begin{array}{c|c}\frac{\bar{\gamma}_1}{(\beta-\delta)\bar{\gamma}_{3,i}} & -N_d-d+l,-N_d-d+l \\ & 1,d-l,1 \\ \frac{\bar{\gamma}_2}{\bar{\gamma}_{4,j}} & -d+l-N_d \\ & d-l,1+d-l,d,N_d+1,N_d+1\end{array}\right]. \tag{24}$$

with $\mathrm{G}_{2,[2:1],1,[3:2]}^{2,1,1,3,2}\left[\cdot\,|\cdot\right]$ *being the Meijer-G functions with two variables.*

Proof. See Appendix B. □

Finally, by substituting (18), (19) and (22) into (14), one can directly calculate the ergodic capacity of the considered hybrid network.

Remark 1. *Note that the Meijer-G function of single variable can be efficiently calculated by some computing softwares, such as Matlab and Mathematic, and the Meijer-G functions of two variables can be alternatively computed by using an efficient approach proposed in [31]-[32], thus our theoretical formula provides an efficient method to evaluate the performance of the HSTRNs.*

B. Outage Probability

The OP is an important quality-of-service (QoS) measure in wireless systems and is defined as the probability that the output instantaneous SNR γ_d falls below an acceptable SNR threshold γ_{th}, namely, [7]-[8]

$$\Pr\left(\gamma_d\leq\gamma_{th}\right)=F_{\gamma_d}\left(\gamma_{th}\right). \tag{25}$$

The CDF $F_{\gamma_d}\left(\gamma_{th}\right)$ of γ_d in (4) is mathematically intractable. To overcome this problem, we consider the upper bound of the instantaneous end-to-end SINR in (4) as [23]

$$\gamma_d\leq\gamma_{up}=\min\left(\Gamma_1,\Gamma_2\right). \tag{26}$$

Then, the CDF of γ_{up} can be obtained as

$$F_{\gamma_{up}}\left(x\right)=1-\left[1-F_{\Gamma_1}\left(x\right)\right]\left[1-F_{\Gamma_2}\left(x\right)\right], \tag{27}$$

where the CDFs, $F_{\Gamma_1}\left(x\right)$ and $F_{\Gamma_2}\left(x\right)$, can be approximated as

$$F_{\Gamma_1}\left(x\right)\approx\int_0^\infty F_{\gamma_1}\left(xz\right)f_{\gamma_3}\left(z\right)dz, \tag{28}$$

$$F_{\Gamma_2}\left(x\right)\approx\int_0^\infty F_{\gamma_2}\left(xz\right)f_{\gamma_4}\left(z\right)dz, \tag{29}$$

In (28) and (29), we have exploited the fact that the considered system is interference limited, and the noise term is omitted in (16) and (17). It will be demonstrated in Section IV through the computer simulations that although there exist a small deviation at low SNR, the approximated approach in (26) can provide sufficient accuracy.

By substituting (6) and (9) into (28), $F_{\Gamma_1}(x)$ can be computed as

$$F_{\Gamma_1}(x) = \alpha^{N_s} \sum_{l=0}^{c} \binom{c}{l} \beta^{c-l} \sum_{i=1}^{I_1} \frac{\rho_i}{\bar{\gamma}_{3,i}} \left(\frac{(\beta-\delta)^{\frac{l-d-1}{2}} x^{\frac{d-l-1}{2}}}{\bar{\gamma}_1^{\frac{d-l-1}{2}} \Gamma(d-l+1)} \right. \\ \times \int_0^\infty z^{\frac{d-l-1}{2}} e^{-\left(\frac{(\beta-\delta)x}{2\bar{\gamma}_1} + \frac{1}{\bar{\gamma}_{3,i}}\right) z} M_{\frac{d+l-1}{2}, \frac{d-l}{2}} \left(\frac{\beta-\delta}{\bar{\gamma}_1} xz \right) dz \\ \left. + \frac{\varepsilon\delta(\beta-\delta)^{\frac{l-d}{2}} x^{\frac{d-l}{2}}}{\bar{\gamma}_1^{\frac{d-l}{2}} \Gamma(d-l+2)} \int_0^\infty z^{\frac{d-l}{2}} e^{-\left(\frac{(\beta-\delta)x}{2\bar{\gamma}_1} + \frac{1}{\bar{\gamma}_{3,i}}\right) z} M_{\frac{d+l}{2}, \frac{d-l+1}{2}} \left(\frac{\beta-\delta}{\bar{\gamma}_1} xz \right) dz \right). \tag{30}$$

Then, by utilizing [26, eq. (7.621.2)] and [33, eq. (10)], (30) can be obtained as

$$F_{\Gamma_1}(x) = \alpha^{N_s} \sum_{l=0}^{c} \binom{c}{l} \beta^{c-l} \sum_{i=1}^{I_1} \rho_i \left(\frac{1}{\Gamma(d)} \left(\frac{\bar{\gamma}_{3,i} x}{\bar{\gamma}_1} \right)^{d-l} \mathrm{G}_{1,1}^{1,1} \left[\frac{(\beta-\delta)\bar{\gamma}_{3,i}}{\bar{\gamma}_1} x \middle| \begin{matrix} 1-d \\ 0 \end{matrix} \right] \right. \\ \left. + \frac{\varepsilon\delta(\beta-\delta)}{\Gamma(d+1)} \left(\frac{\bar{\gamma}_{3,i} x}{\bar{\gamma}_1} \right)^{d-l+1} \mathrm{G}_{1,1}^{1,1} \left[\frac{(\beta-\delta)\bar{\gamma}_{3,i}}{\bar{\gamma}_1} x \middle| \begin{matrix} -d \\ 0 \end{matrix} \right] \right). \tag{31}$$

Similarly, by substituting (8) and (11) into (29) yields

$$F_{\Gamma_2}(x) = 1 - \sum_{i=0}^{N_d-1} \frac{1}{i!} \left(\frac{x}{\bar{\gamma}_2} \right)^i \sum_{j=1}^{I_2} \frac{\omega_j}{\bar{\gamma}_{4,j}} \int_0^\infty z^i e^{-\left(\frac{x}{\bar{\gamma}_2} + \frac{1}{\bar{\gamma}_{4,j}}\right) z} dz. \tag{32}$$

Thus, with the help of [26, eq. (3.351.3)] and [33, eq. (10)], $F_{\Gamma_2}(x)$ can be calculated as

$$F_{\Gamma_2}(x) = 1 - \sum_{i=0}^{N_d-1} \frac{1}{i!} \left(\frac{x}{\bar{\gamma}_2} \right)^i \sum_{j=1}^{I_2} \omega_j \bar{\gamma}_{4,j}^i \mathrm{G}_{1,1}^{1,1} \left[\frac{\bar{\gamma}_{4,j} x}{\bar{\gamma}_2} \middle| \begin{matrix} -i \\ 0 \end{matrix} \right]. \tag{33}$$

Finally, by substituting (31) and (33) into (27), after some algebraic manipulations, $F_{\gamma_{up}}(x)$ can be expressed as

$$F_{\gamma_{up}}(x) = 1 - \sum_{k=0}^{N_d-1} \frac{1}{k!} \left(\frac{x}{\bar{\gamma}_2} \right)^k \sum_{j=1}^{I_2} \omega_j \bar{\gamma}_{4,j}^i \mathrm{G}_{1,1}^{1,1} \left[\frac{\bar{\gamma}_{4,j} x}{\bar{\gamma}_2} \middle| \begin{matrix} -k \\ 0 \end{matrix} \right] + \alpha_s^N \sum_{l=0}^{c} \binom{c}{l} \beta^{c-l} \sum_{i=1}^{I_1} \rho_i \sum_{i=0}^{N_d-1} \frac{1}{i!} \left(\frac{x}{\bar{\gamma}_2} \right)^k \\ \times \sum_{j=1}^{I_2} \rho_j \bar{\gamma}_{4,j}^i \mathrm{G}_{1,1}^{1,1} \left[\frac{\bar{\gamma}_{4,j} x}{\bar{\gamma}_2} \middle| \begin{matrix} -k \\ 0 \end{matrix} \right] \left(\frac{1}{\Gamma(d)} \left(\frac{\bar{\gamma}_{3,i} x}{\bar{\gamma}_1} \right)^{d-l} \mathrm{G}_{1,1}^{1,1} \left[\frac{(\beta-\delta)\bar{\gamma}_{3,i}}{\bar{\gamma}_1} x \middle| \begin{matrix} 1-d \\ 0 \end{matrix} \right] \right. \\ \left. + \frac{\varepsilon\delta(\beta-\delta)}{\Gamma(d+1)} \left(\frac{\bar{\gamma}_{3,i} x}{\bar{\gamma}_1} \right)^{d-l+1} \mathrm{G}_{1,1}^{1,1} \left[\frac{(\beta-\delta)\bar{\gamma}_{3,i}}{\bar{\gamma}_1} x \middle| \begin{matrix} -d \\ 0 \end{matrix} \right] \right). \tag{34}$$

To this end, by replacing x with γ_{th} in (34), it is straightforward to calculate the approximated yet accurate OP of the considered HSTRH in the presence of CCIs.

C. Average Symbol Error Rate

According to [34], by using the MGF, the ASER expression of wireless systems over fading channels can be expressed as

$$P_e = \sum \int_0^{\theta} a M_{\gamma_d}\left(\frac{b}{\sin^2\phi}\right) d\phi, \tag{35}$$

where a, b and θ are the modulation specific parameters, such as $(a=1, b=1)$ for binary phase shift keying (BPSK), $\left(a=2, b=\sin^2(\pi/M)\right)$ for M-ary phase shift keying (M-PSK) $(M \geq 4)$, and $(a=2(M-1)/M, b=3/(M^2-1))$ for M-ary pulse amplitude modulation (M-PAM).

Using (34) and (21), $M_{\gamma_d}(x)$ can be computed as [36]

$$\begin{aligned} M_{\gamma_d}(s) &\approx \int_0^{\infty} s e^{-sx} F_{\gamma_{up}}(x)\, dx \\ &= 1 - s \sum_{k=0}^{N_d-1} \frac{1}{k!\bar{\gamma}_2^k} \sum_{j=1}^{I_2} \omega_j \bar{\gamma}_{4,j}^k \underbrace{\int_0^{\infty} x^k e^{-sx} \mathrm{G}_{1,1}^{1,1}\left[\frac{\bar{\gamma}_{4,j}x}{\bar{\gamma}_2}\middle| \begin{matrix} -k \\ 0 \end{matrix}\right] dx}_{I_1} \\ &\quad + s\alpha^{N_s} \sum_{l=0}^{c} \binom{c}{l} \beta^{c-l} \sum_{i=1}^{I_1} \rho_i \sum_{k=0}^{N_d-1} \frac{1}{k!\bar{\gamma}_2^k} \sum_{j=1}^{I_2} \omega_j \bar{\gamma}_{4,j}^k \\ &\times \Bigg(\frac{1}{\Gamma(d)} \left(\frac{\bar{\gamma}_{3,i}}{\bar{\gamma}_1}\right)^{d-l} \underbrace{\int_0^{\infty} x^{d-l+k} e^{-sx} \mathrm{G}_{1,1}^{1,1}\left[\frac{\bar{\gamma}_{4,j}x}{\bar{\gamma}_2}\middle| \begin{matrix} -k \\ 0 \end{matrix}\right] \mathrm{G}_{1,1}^{1,1}\left[\frac{(\beta-\delta)\bar{\gamma}_{3,i}}{\bar{\gamma}_1}x\middle| \begin{matrix} 1-d \\ 0 \end{matrix}\right] dx}_{I_2} \\ &\quad + \frac{\varepsilon\delta(\beta-\delta)}{\Gamma(d+1)} \left(\frac{\bar{\gamma}_{3,i}}{\bar{\gamma}_1}\right)^{d-l+1} \underbrace{\int_0^{\infty} x^{d-l+k+1} e^{-sx} \mathrm{G}_{1,1}^{1,1}\left[\frac{\bar{\gamma}_{4,j}x}{\bar{\gamma}_2}\middle| \begin{matrix} -k \\ 0 \end{matrix}\right] \mathrm{G}_{1,1}^{1,1}\left[\frac{(\beta-\delta)\bar{\gamma}_{3,i}}{\bar{\gamma}_1}x\middle| \begin{matrix} -d \\ 0 \end{matrix}\right] ds}_{I_3} \Bigg). \end{aligned} \tag{36}$$

As for the first integral I_1, by using [26, eq. (7.813.1)], it can be written as

$$I_1 = s^{-k-2} \mathrm{G}_{2,1}^{1,2}\left[\frac{\bar{\gamma}_{4,j}}{\bar{\gamma}_2 s}\middle| \begin{matrix} -k-1, -k \\ 0 \end{matrix}\right]. \tag{37}$$

Then, to solve the other two integrals I_2 and I_3, we express the exponential function in terms

of Meijer-G function as [33, eq. (11)]

$$e^{-sx}=\mathrm{G}_{0,1}^{1,0}\left[sx\left|\begin{matrix}-\\0\end{matrix}\right.\right]. \tag{38}$$

By substituting (38) into I_2 and I_3, and applying the identity in [27, eq. (3.1)], we have

$$I_2 = s^{-d+l-k-1}L\left(i,j,d,l,k\right), \tag{39}$$

and

$$I_3 = s^{-d+l-k-2}L\left(i,j,d+1,l,k\right), \tag{40}$$

where

$$L\left(i,j,d,l,k\right)=\mathrm{G}_{1,[1:1],0,[1:1]}^{1,1,1,1,1}\left[\begin{matrix}\frac{\bar{\gamma}_1}{(\beta-\delta)\bar{\gamma}_{3,i}}\\ \frac{\bar{\gamma}_2}{\bar{\gamma}_{4,j}}\end{matrix}\middle|\begin{matrix}d-l+k+1\\ -d+1;-k\\ -;-\\ 0,0\end{matrix}\right]. \tag{41}$$

By using I_1, I_2 and I_3 into (36), the analytical expression of M_{γ_d} can be obtained as

$$\begin{aligned}M_{\gamma_d}\left(s\right)\approx 1-\sum_{k=0}^{N_d-1}\frac{s^{-k-1}}{k!\bar{\gamma}_2^k}\sum_{j=1}^{I_2}\omega_j\bar{\gamma}_{4,j}^k\mathrm{G}_{2,1}^{1,2}\left[\frac{\bar{\gamma}_{4,j}}{\bar{\gamma}_2 s}\middle|\begin{matrix}-k-1,-k\\0\end{matrix}\right]+\alpha^{N_s}\sum_{l=0}^{c}\binom{c}{l}\beta^{c-l}\sum_{i=1}^{I_1}\rho_i\\ \times\sum_{k=0}^{N_d-1}\frac{1}{k!\bar{\gamma}_2^k}\sum_{j=1}^{I_2}\omega_j\bar{\gamma}_{4,j}^k\left(\frac{s^{-d+l-k}}{\Gamma\left(d\right)}\left(\frac{\bar{\gamma}_{3,i}}{\bar{\gamma}_1}\right)^{d-l}L\left(i,j,d,l,k\right)\right.\\ \left.+\frac{\varepsilon\delta\left(\beta-\delta\right)s^{-d+l-k-1}}{\Gamma\left(d+1\right)}\left(\frac{\bar{\gamma}_{3,i}}{\bar{\gamma}_1}\right)^{d-l+1}L\left(i,j,d+1,l,k\right)\right).\end{aligned} \tag{42}$$

In what follows, we provide an approximate yet accurate ASER expressions in terms of three commonly used modulation formats, namely, M-PAM, M-PSK, and M-ary quadrature amplitude modulation (M-QAM),

First of all, for the M-PAM modulation signals, the ASER can be calculated as [34]

$$P_{M-\mathrm{PAM}}\approx 2\left(\frac{M-1}{\pi M}\right)\int_0^{\pi/2}M_{\gamma_d}\left(\frac{3}{(M^2-1)\sin^2\phi}\right)d\phi. \tag{43}$$

Although the ASER of the considered network can be computed by substituting (42) into (43), it requires a numerical integration. To solve this problem, by using [35, eq. (3), eq. (14)], an alternative method is given by

$$P_{M-\mathrm{PAM}}\approx\frac{2\left(M-1\right)}{M}\left[\frac{1}{12}M_{\gamma_d}\left(\frac{3}{M^2-1}\right)+\frac{1}{4}M_{\gamma_d}\left(\frac{4}{M^2-1}\right)\right]. \tag{44}$$

For M-PSK modulation signals, the ASER can be obtained as [34]

$$P_{M-\mathrm{PSK}} = \frac{1}{\pi}\int_0^{(M-1)\pi/M} M_{\gamma_d}\left(\frac{\sin^2(\pi/M)}{\sin^2\phi}\right)d\phi, \tag{45}$$

which can be approximated as

$$\begin{aligned} P_{M-\mathrm{PSK}} \approx & \left(\frac{M-1}{2M}-\frac{1}{6}\right)M_{\gamma_d}\left(\sin^2\left(\frac{\pi}{M}\right)\right)+\frac{1}{4}M_{\gamma_d}\left(\frac{4}{3}\sin^2\left(\frac{\pi}{M}\right)\right) \\ & +\left(\frac{M-1}{2M}-\frac{1}{4}\right)M_{\gamma_d}\left(\frac{\sin^2(\pi/M)}{\sin^2((M-1)\pi/M)}\right). \end{aligned} \tag{46}$$

For a square M-QAM modulation signal, since it can be considered as two independent $\sqrt{M}$-PAM signals, its ASER can be evaluated as [34]

$$\begin{aligned} P_{M-\mathrm{QAM}} = & \frac{4}{\pi}\left(1-\frac{1}{\sqrt{M}}\right)\int_0^{\pi/2} M_{\gamma_d}\left(\frac{3}{(M-1)\sin^2\phi}\right)d\phi \\ & +\frac{4}{\pi}\left(1-\frac{1}{\sqrt{M}}\right)^2\int_0^{\pi/4} M_{\gamma_d}\left(\frac{3}{(M-1)\sin^2\phi}\right)d\phi. \end{aligned} \tag{47}$$

Following a similar derivation to (44) and (46), the approximate expression of $P_{M-\mathrm{QAM}}$ can be calculated as

$$\begin{aligned} P_{M-\mathrm{QAM}} \approx & \left(\frac{1}{\sqrt{M}}-\frac{1}{M}\right)\left(\frac{1}{3}M_{\gamma_d}\left(\frac{3}{M-1}\right)+M_{\gamma_d}\left(\frac{4}{M-1}\right)\right) \\ & +\frac{1}{2}\left(1-\frac{1}{\sqrt{M}}\right)^2\left(M_{\gamma_d}\left(\frac{6}{M-1}\right)-M_{\gamma_d}\left(\frac{3}{M-1}\right)\right). \end{aligned} \tag{48}$$

Remark 2. *It should be pointed out that although the approximate formulas are derived to calculate the ASER performance of the HSTRNs with various modulation formats, computer simulations in Section IV will demonstrate that the proposed method can provide satisfied accuracy.*

D. Asymptotic Analysis at High SNR

In this section, we provide the asymptotic analysis at high SNR in terms of diversity order and array gain to gain further insights into the considered network.

First of all, inspired by [14] and [29], by using the the series representation of Meijer-G function as [37, eq. (9.303)]

$$\mathrm{G}_{p,q}^{m,n}\left[x\left|\begin{matrix}a_1,\ldots,a_p\\ b_1,\ldots,b_q\end{matrix}\right.\right] = \sum_{h=1}^{m}\frac{\prod_{j=1,j\neq h}^{m}\Gamma\left(b_j-b_h\right)\prod_{j=1}^{n}\Gamma\left(1-b_h-a_j\right)}{\prod_{j=m+1}^{q}\Gamma\left(1+b_h-b_j\right)\prod_{j=n+1}^{p}\Gamma\left(a_j-b_h\right)}x^{b_h}$$

$$\times {}_pF_q\left(1+b_h-a_1,\ldots,1+b_h-a_p;1+b_h-b_1,\ldots,1+b_h-b_q;(-1)^{p-m-n}x\right), \tag{49}$$

where in the case of $x \to 0$, ${}_pF_q\left(;;\right)$ has the property as [38]

$$ {}_pF_q\left(a_1,\ldots,a_p;b_1,\ldots,b_q;x\right) \to 1, \tag{50}$$

the asymptotic CDF of Γ_1 can be expressed as

$$F_{\Gamma_1}^{\infty}\left(x\right) = \alpha^{N_s}\sum_{l=0}^{c}\left(\begin{array}{c} c \\ l \end{array}\right)\beta^{c-l}\sum_{i=1}^{I_1}\eta_i\left(\frac{\bar{\gamma}_{3,i}x}{\bar{\gamma}_1}\right)^{d-l}. \tag{51}$$

Considering that asymptotic performance of $F_{\Gamma_1}^{\infty}\left(x\right)$ is determined by the lowest terms of $\bar{\gamma}_1$ at high SNR, we let $l = c$ in (51), and further obtain

$$F_{\Gamma_1}^{\infty}\left(x\right) = \alpha^{N_s}\sum_{i=1}^{I_1}\rho_i\left(\frac{\bar{\gamma}_{3,i}x}{\bar{\gamma}_1}\right)^{N_s} + O\left(x^{N_s+1}\right), \tag{52}$$

where $O\left(\cdot\right)$ stands for higher order terms. Meanwhile, as for $F_{\gamma_2}^{\infty}\left(x\right)$, by applying the Maclaurin series representation of exponential function to (8), one can obtain

$$F_{\gamma_2}^{\infty}\left(x\right) = \frac{1}{N_d!}\left(\frac{x}{\bar{\gamma}_2}\right)^{N_d} + O\left(x^{N_d+1}\right). \tag{53}$$

Hence, by using (53) and (11) along with [26, eq. (3.351.3)], the CDF of Γ_2 in (29) at high SNR is given by

$$F_{\Gamma_2}^{\infty}\left(x\right) = \frac{1}{\bar{\gamma}_2^{N_d}}\sum_{j=1}^{I_2}\omega_j\bar{\gamma}_{4,j}^{N_d}x^{N_d} + O\left(x^{N_d+1}\right). \tag{54}$$

Finally, substituting (52) and (54) into (27) yields the $F_{\gamma_{up}}^{\infty}\left(x\right)$ as

$$F_{\gamma_{up}}^{\infty}\left(x\right) = \begin{cases} \alpha^{N_s}\sum\limits_{i=1}^{I_1}\rho_i\left(\frac{\bar{\gamma}_{3,i}}{\bar{\gamma}_1}\right)^{N_s}x^{N_s}, & N_s < N_d \\ \left[\alpha^{N_{eq}}\sum\limits_{i=1}^{I_1}\rho_i\left(\frac{\bar{\gamma}_{3,i}}{\bar{\gamma}_1}\right)^{N_{eq}} + \sum\limits_{j=1}^{I_2}\omega_j\left(\frac{\bar{\gamma}_{4,j}}{\bar{\gamma}_2}\right)^{N_d}\right]x^{N_{eq}}, & N_s = N_d = N_{eq} \\ \sum\limits_{j=1}^{I_2}\omega_j\left(\frac{\bar{\gamma}_{4,j}}{\bar{\gamma}_2}\right)^{N_d}, & N_s > N_d \end{cases}. \tag{55}$$

In what follows, we consider the asymptotic behavior of ASER in high SNR regime. To this end, we first denote $\bar{\gamma}_1 = \eta_1\bar{\gamma}$ and $\bar{\gamma}_2 = \eta_2\bar{\gamma}$, and substitute (55) into (21). After some necessary mathematical manipulation, one can obtain

$$M_{\gamma_{up}}^{\infty}\left(s\right) = \begin{cases} \alpha^{N_s}\sum\limits_{i=1}^{I_1}\rho_i\left(\frac{\bar{\gamma}_{3,i}}{\eta_1}\right)^{N_s}\frac{1}{(\bar{\gamma}s)^{N_s}}, & N_s < N_d \\ \left[\alpha^{N_{eq}}\sum\limits_{i=1}^{I_1}\rho_i\left(\frac{\bar{\gamma}_{3,i}}{\eta_1}\right)^{N_{eq}} + \sum\limits_{j=1}^{I_2}\omega_j\left(\frac{\bar{\gamma}_{4,j}}{\eta_2}\right)^{N_{eq}}\right]\frac{1}{(\bar{\gamma}s)^{N_{eq}}}, & N_s = N_d = N_{eq} \\ \sum\limits_{j=1}^{I_2}\omega_j\left(\frac{\bar{\gamma}_{4,j}}{\eta_2}\right)^{N_d}\frac{1}{(\bar{\gamma}s)^{N_d}}, & N_d > N_s \end{cases}. \tag{56}$$

Then, by employing (56) into (35), the asymptotic ASER expression with respect to the diversity order and array gain can be obtained as

$$P_s^{\infty} = \left(G_a \bar{\gamma}\right)^{-G_d} + O\left(\bar{\gamma}^{-\left(G_d+1\right)}\right), \tag{57}$$

where the diversity order and array gain are given by

$$G_d = \min\left(N_s, N_d\right), \tag{58}$$

and

$$G_a = \begin{cases} \Xi\left(a,b,\theta\right)\alpha^{N_s}\sum\limits_{i=1}^{I_1}\rho_i\left(\frac{\bar{\gamma}_{3,i}}{\eta_1}\right)^{N_s}, & N_s < N_d \\ \Xi\left(a,b,\theta\right)\left[\alpha^{N_{eq}}\sum\limits_{i=1}^{I_1}\rho_i\left(\frac{\bar{\gamma}_{3,i}}{\eta_1}\right)^{N_{eq}} + \frac{1}{N_{eq}!\eta_2^{N_{eq}}}\right], & N_s = N_d = N_{eq} \\ \Xi\left(a,b,\theta\right)\sum\limits_{j=1}^{I_2}\omega_j\left(\frac{\bar{\gamma}_{4,j}}{\eta_2}\right)^{N_d}, & N_d < N_s \end{cases}, \tag{59}$$

where $\Xi\left(a,b,\theta\right)$ is determined by the modulation formats, which will be described as follows.

1) M-PAM: In the case of M-PAM modulation, $\Xi\left(a,b,\theta\right)$ can be written as

$$\Xi\left(a,b,\theta\right) = \frac{2\left(M-1\right)/\pi M}{\left(3/\left(M^2-1\right)\right)^{2G_d}}\int_0^{\pi/2}\left(\sin\phi\right)^{2G_d}d\phi. \tag{60}$$

By using [26, eq. (3.621.3)] and [38, eq. (6.1.49)], (60) can be rewritten as

$$\Xi\left(a,b,\theta\right) = \frac{2\left(M-1\right)/\pi M}{\left(3/\left(M^2-1\right)\right)^{2G_d}}\frac{\sqrt{\pi}\Gamma\left(G_d+1/2\right)}{2\Gamma\left(G_d\right)}. \tag{61}$$

2) M-PSK: For the M-PSK modulation, $\Xi\left(a,b,\theta\right)$ can be expressed as

$$\Xi\left(a,b,\theta\right) = \frac{1}{\left(\sin\left(\pi/M\right)\right)^{2G_d}}\int_0^{\pi-\pi/M}\left(\sin\phi\right)^{2G_d}d\phi. \tag{62}$$

Applying [26, eq. (3.621.3)] and [38, eq. (6.1.49)] along with the symmetry and periodicity of the sine function, we can obtain

$$\begin{aligned}\Xi\left(a,b,\theta\right) &= \frac{1}{\left(\sin\left(\pi/M\right)\right)^{2N}}\left(\int_0^{\pi/2}\left(\sin\phi\right)^{2G_d}d\phi + \int_{\pi/M}^{\pi/2}\left(\sin\phi\right)^{2G_d}d\phi\right) \\ &= \frac{1}{\pi\sin^{2G_d}\left(\pi/M\right)}\left(\frac{\sqrt{\pi}\Gamma\left(G_d+1/2\right)}{2\Gamma\left(G_d\right)} + \cos\left(\frac{\pi}{M}\right){}_2F_1\left(\frac{1}{2},-G_d-\frac{1}{2};\frac{3}{2};\cos^2\left(\frac{\pi}{M}\right)\right)\right),\end{aligned} \tag{63}$$

where ${}_2F_1\left(a,b;c;z\right)$ denotes the Gauss hypergeometric function [26].

3) M-QAM: Similar to the procedures in deriving (63), $\Xi\left(a,b,\theta\right)$ for M-QAM modulation is given by

$$\Xi\left(a,b,\theta\right) = \frac{4}{\pi}\left(\frac{1}{\sqrt{M}}-\frac{1}{M}\right)\left(\frac{M-1}{3}\right)^{2G_d}\int_0^{\pi/2}\left(\sin\phi\right)^{2G_d}d\phi$$

$$+\frac{4}{\pi}\left(1-\frac{1}{\sqrt{M}}\right)^{2}\left(\frac{M-1}{3}\right)^{2G_d}\int_{\pi/4}^{\pi/2}(\sin\phi)^{2G_d}\,d\phi$$
$$=\frac{4}{\pi}\left(\frac{1}{\sqrt{M}}-\frac{1}{M}\right)\left(\frac{M-1}{3}\right)^{2G_d}\frac{\sqrt{\pi}\Gamma\left(G_d+1/2\right)}{2\Gamma\left(G_d\right)}$$
$$+\frac{4}{\pi}\left(1-\frac{1}{\sqrt{M}}\right)^{2}\left(\frac{M-1}{3}\right)^{2G_d}+\frac{\sqrt{2}}{2}{}_2F_1\left(\frac{1}{2},-G_d-\frac{1}{2};\frac{3}{2};\frac{1}{2}\right). \quad (64)$$

Remark 3. *It is revealed in (58) that the maximal achievable diversity order of the considered HSTRN equals the minimal number of the antennas deployed at the source and destination. Moreover, it can also be observed from (59) that although the CCIs do not affect the system diversity order, they do degrade the performance of HSTRN through reducing the array gain.*

V. Numerical Results

This section presents computer simulations to confirm the validity of the presented analytical results and investigates the impact of the system parameters on the performance of the considered HSTRN. In the simulation, the satellite-relay link is subject to Shadowed-Rician fading with channel parameters shown in Table I, and the relay-destination link follows Rayleigh fading distribution. Similar to most of the related works, we consider $\eta_1 = \eta_2 = 1$, namely, $\bar{\gamma}_1 = \bar{\gamma}_2 = \bar{\gamma}$, and equal total CCI power at the relay and destination, namely, $\sum_{i=1}^{I_1}\bar{\gamma}_{3,i} = \sum_{j=1}^{I_2}\bar{\gamma}_{4,j} = \bar{\gamma}_{tot}$. In addition, the label (N_s, N_d) denotes the number of antennas at the source and destination, respectively, and all the simulations are obtained by performing 10^7 channel realizations.

Fig. 2 shows the ergodic capacity of the HSTRN for different antenna configurations, where the satellite-relay link undergoes the average shadowing (AS) and $I_1 = I_2 = 1$ with $\bar{\gamma}_{tot} = 1$dB. It can be seen from Fig. 2 that the proposed analytical results are in good agreement with the simulation results, implying the proposed expressions can accurately evaluate the ergodic capacity of the considered system. Meanwhile, as we expect, the ergodic capacity improves with the increase of number of antennas, demonstrating the benefits of employing multiple antennas and beamforming in HSTRNs. For example, the antenna configuration with $(N_s, N_d) = (4, 4)$ can achieve a capacity enhancement of approximate 1bits/s/Hz in comparison with $(N_s, N_d) = (2, 2)$ at $\bar{\gamma} = 30$dB. In addition, Fig. 3 shows the impact of different CCI powers on the ergodic capacity of the HSTRN for the other fading cases, namely, frequent heavy shadowing (FHS) and infrequent light shadowing (ILS). Here, we assume $(N_s, N_d) = (4, 4)$, $\bar{\gamma}_{tot} = \{-\infty, 1, 3\}$dB with $\bar{\gamma}_{tot} = -\infty$dB denote the case of no CCI, and $I_1 = I_2 = 2$ with $\bar{\gamma}_{3,1} = 2\bar{\gamma}_{3,2}$ and $\bar{\gamma}_{4,1} = 2\bar{\gamma}_{4,2}$.

TABLE I: LMS Channel Parameters [4]

Shadowing	b	m	Ω
Frequent heavy shadowing (FHS)	0.063	0.739	8.97×10^{-4}
Average shadowing (AS)	0.126	10.1	0.835
Infrequent light shadowing (ILS)	0.158	19.4	1.29

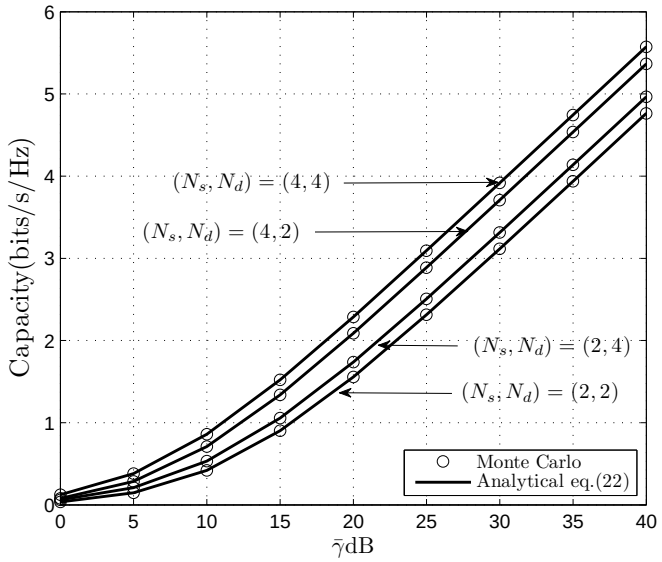

Fig. 2: Ergodic capacity versus $\bar{\gamma}$ for various antenna configurations.

It can be seen from Fig. 3 that for both the FHS and ILS scenarios, the increase of the CCI powers cause noticeable degradation on the system capacity. However, as the CCI power increases, the capacity gap between FHS and ILS becomes smaller, which indicates that in the presence of strong interference, the ergodic capacity is not sensitive to the shadowing conditions.

Fig. 4 illustrates the OP of HSTRN with different antenna configurations for the threshold $\gamma_{th} = 3$dB and $I_1 = I_2 = 1$ with $\bar{\gamma}_{tot} = 1$dB. The curves of the analytical OP and that of asymptotic OP are calculated by (34) and (55), respectively. As illustrated, an excellent agreement between the simulation and analytical results can be seen, and the analytical curve is sufficiently tight across the entire SNR range of interest, while the asymptotic curves match well with the exact curves at high SNR. In addition, increasing the number of antennas at the source and/or destination significantly degrades the system OP. Moreover, it can be clearly seen that the achievable diversity order of the considered system equals to the minimal antenna number

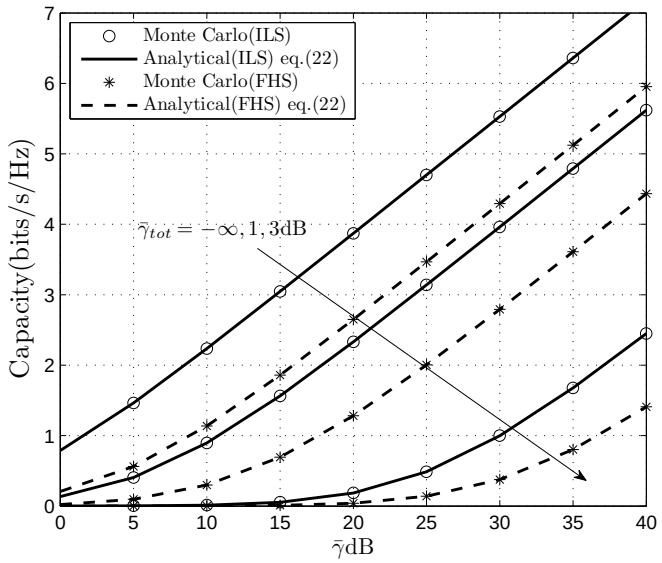

Fig. 3: Ergodic capacity versus $\bar{\gamma}$ for various CCI powers.

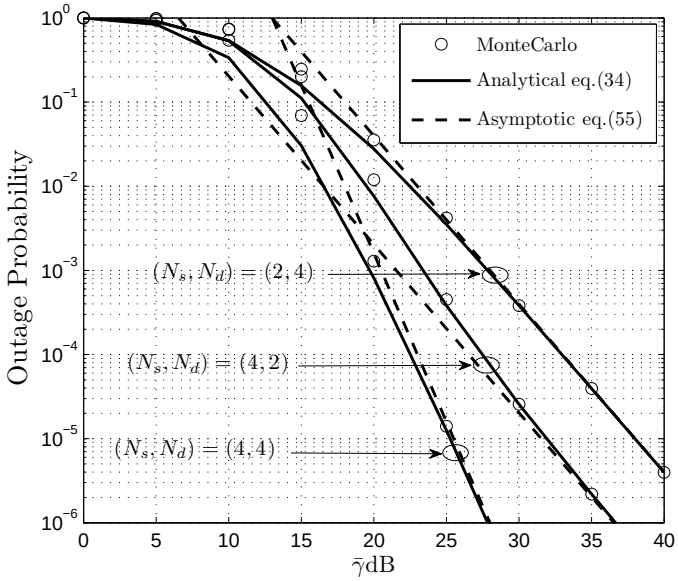

Fig. 4: Outage probability of HSTRN for different antenna configurations.

deployed at source and destination, or mathematically, $\min(N_s, N_d)$. For example, the diversity order is two for the configurations $(N_s, N_d) = (4, 2)$ and $(N_s, N_d) = (2, 4)$, and four for the configuration $(N_s, N_d) = (4, 4)$.

Fig. 5 depicts the ASER of HSTRN with different antenna configurations for BPSK and 8PSK modulation schemes. As seen from the figure, the analytical ASER curves are very closed to

the simulation results at high SNR regime. Moreover, asymptotic ASER curves in (57) are also plotted to provide further insights into the diversity order and array gain under different antenna configurations. Just as in the case of OP, it can be seen that the more antennas are employed at the source and/or destination, the better system performance can be achieved. Moreover, it can be observed that the configuration with $(N_s, N_d) = (4, 2)$ exhibits a better ASER performance than that with $(N_s, N_d) = (2, 4)$, which indicates the antennas employed at the source pose a greater influence on the system performance than the antennas at the destination. This is due to the fact that, by employing the AF protocol, the SINR of the S-R link is amplified by the relay node. This observation also suggests that, if the total available number of antennas is fixed, more antennas should be deployed at the source. Fig. 6 plots the ASER curves of HSTRN for different CCI powers with BPSK modulation scheme, where the simulation parameters are set the same as Fig. 2. Similar to the cases of ergodic capacity, with the increase of CCI power, the ASER performance degrades significantly, which demonstrates the detrimental effect of the interference. When the CCI power increases from $-\infty$ to 3dB, although the diversity order of the considered network remains four, the significant performance degradation occurs. This is because the CCI causes the loss of array gain. Furthermore, from the ASER comparison between FHS and AS scenarios, although the AS case outperform the FHS case, the better channel quality does not offer any additional diversity order. However, it does improve the system performance by providing extra array gain.

VI. Conclusions

In this paper, we have investigated the performance of the multiple antenna hybrid satellite-terrestrial relay network with multiple co-channel interferes at both the terrestrial relay and destination. Specifically, the approximated closed-form expression for ergodic capacity of the considered networks has first been derived. Then, we have obtained the analytical expressions of OP and ASER, which is very tight in general despite a little deviation in low SNR regime. Moreover, the simple asymptotic formulas at high SNR regime have also been provided, which enables the characterization of various system parameters on the achievable diversity order and array gain of the considered network. Simulations have been provided to confirm the validity of the theoretical analysis, and indicated the impact of key system parameters, such as antenna number, channel coefficients and CCI power on the system performance. It has been found that

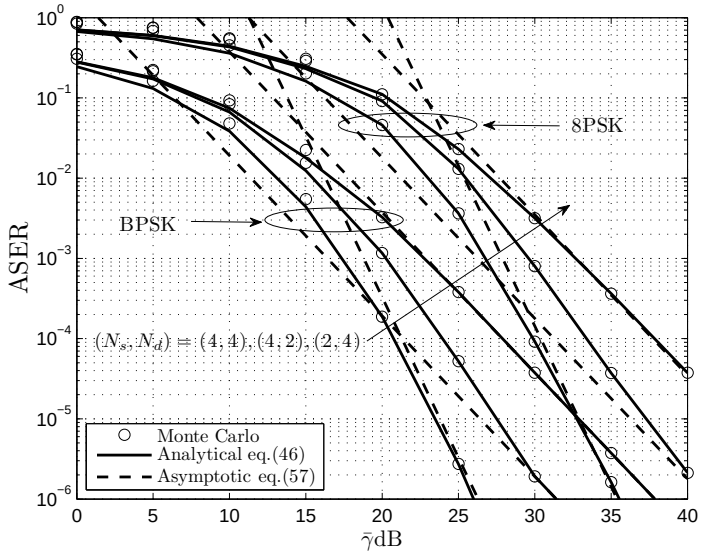

Fig. 5: Average symbol error rate of HSTRN for different antenna configurations in terms of BPSK and 8PSK modulation formats.

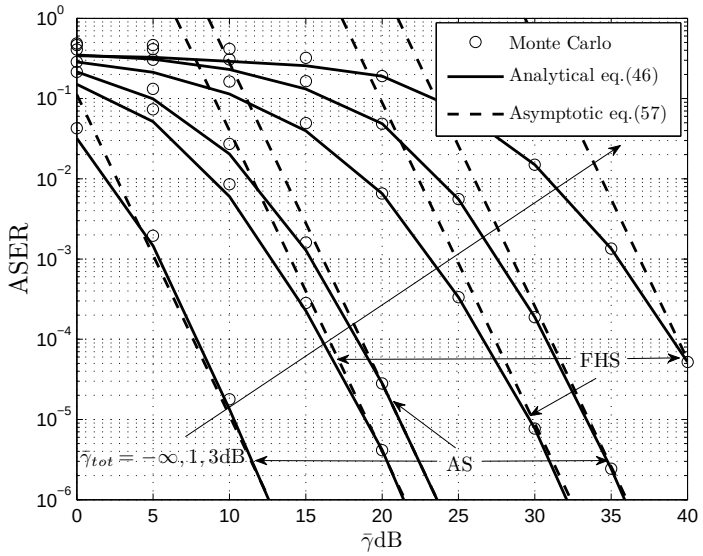

Fig. 6: Average symbol error rate of HSTRN for different CCI powers in terms of BPSK modulation format.

although the maximal diversity of $\min(N_s, N_d)$ can be achieved, the CCI severely degrades the performance of HSTRN by reducing the array gain.

ACKNOWLEDGMENT

This work is supported by the National Natural Science Foundation of China under Grant 61271255 and the Natural Science Foundation of Jiangsu Province under Grant BK20131068.

APPENDIX A
PROOF OF THEOREM 1

From (16) and (17), in order to obtain $C_i\,(i=1,2)$, we first calculate $f_{\Gamma_i}(x)\,(i=1,2)$. By substituting (5) and (9) into (16), we have

$$f_{\Gamma_1}(x)=\alpha^N\sum_{l=0}^{c}\binom{c}{l}\beta^{c-l}\sum_{i=1}^{I_1}\frac{\rho_i}{\bar{\gamma}_{3,i}}\left(\frac{x^{d-l-1}}{\bar{\gamma}_1^{d-l}\Gamma(d-l)}\underbrace{\int_0^\infty z^{d-l}e^{-\frac{z}{\bar{\gamma}_{3,i}}}{}_1F_1\left(d;d-l;-\frac{(\beta-\delta)xz}{\bar{\gamma}_1}\right)dz}_{I_{A,1}}\right.$$
$$\left.+\frac{\varepsilon\delta x^{d-l}}{\bar{\gamma}_1^{d-l+1}\Gamma(d-l+1)}\underbrace{\int_0^\infty z^{d-l+1}e^{-\frac{z}{\bar{\gamma}_{3,i}}}{}_1F_1\left(d+1;d-l+1;-\frac{(\beta-\delta)xz}{\bar{\gamma}_1}\right)dz}_{I_{A,2}}.\right)\quad\text{(A.1)}$$

For the convenience of subsequent derivation, with the help of [26, eq. (8.455.1)], we first express ${}_1F_1\left(d;d-l;-(\beta-\delta)xz/\bar{\gamma}_1\right)$ and ${}_1F_1\left(d+1;d-l+1;-(\beta-\delta)xz/\bar{\gamma}_1\right)$ in terms of Meijer-G function as

$${}_1F_1\left(d;d-l;-\frac{(\beta-\delta)xz}{\bar{\gamma}_1}\right)=\frac{\Gamma(d-l)}{\Gamma(d)}\mathrm{G}_{1,2}^{1,1}\left[\frac{(\beta-\delta)xz}{\bar{\gamma}_1}\middle|\begin{matrix}1-d\\0,1-d+l\end{matrix}\right],\quad\text{(A.2)}$$

$${}_1F_1\left(d+1;d-l+1;-\frac{(\beta-\delta)xz}{\bar{\gamma}_1}\right)=\frac{\Gamma(d-l+1)}{\Gamma(d+1)}\mathrm{G}_{1,2}^{1,1}\left[\frac{(\beta-\delta)xz}{\bar{\gamma}_1}\middle|\begin{matrix}-d\\0,-d+l\end{matrix}\right],\quad\text{(A.3)}$$

and further obtain

$$I_{A,1}=\bar{\gamma}_{3,i}^{d-l+1}\mathrm{G}_{2,2}^{1,2}\left[\frac{(\beta-\delta)\bar{\gamma}_{3,i}x}{\bar{\gamma}_1}\middle|\begin{matrix}-d+l,1-d\\0,1-d+l\end{matrix}\right],\quad\text{(A.4)}$$

$$I_{A,2}=\bar{\gamma}_{3,i}^{d-l+2}\mathrm{G}_{2,2}^{1,2}\left[\frac{(\beta-\delta)\bar{\gamma}_{3,i}x}{\bar{\gamma}_1}\middle|\begin{matrix}-d+l-1,-d\\0,-d+l\end{matrix}\right].\quad\text{(A.5)}$$

In deriving $I_{A,1}$ and $I_{A,2}$, we have applied [26, eq. (9.34.8)]. After some algebraic manipulations, the analytical expression for $f_{\Gamma_1}(x)$ is given by

$$f_{\Gamma_1}(x)=\alpha^{N_s}\sum_{l=0}^{c}\binom{c}{l}\beta^{c-l}\sum_{i=1}^{I_1}\rho_i\left(\frac{x^{d-l-1}\bar{\gamma}_{3,i}^{d-l}}{\bar{\gamma}_1^{d-l}\Gamma(d)}\mathrm{G}_{2,2}^{1,2}\left[\frac{(\beta-\delta)\bar{\gamma}_{3,i}x}{\bar{\gamma}_1}\middle|\begin{matrix}-d+l,1-d\\0,1-d+l\end{matrix}\right]\right)$$

$$+\frac{\varepsilon\delta x^{d-l}\bar{\gamma}_{3,i}^{d-l+1}}{\bar{\gamma}_1^{d-l+1}\Gamma\left(d+1\right)}\mathrm{G}_{2,2}^{1,2}\left[\frac{\left(\beta-\delta\right)\bar{\gamma}_{3,i}x}{\bar{\gamma}_1}\middle|\begin{matrix}-d+l-1,-d\\0,-d+l\end{matrix}\right]\Bigg). \tag{A.6}$$

Then, substituting (A.6) into (15) and expressing $\ln\left(1+x\right)$ in terms of Meijer-G function according to [33, eq. (11)]

$$\ln\left(1+x\right)=\mathrm{G}_{2,2}^{1,2}\left[x\middle|\begin{matrix}1,1\\1,0\end{matrix}\right], \tag{A.7}$$

we have

$$C_1=\frac{\alpha^{N_s}}{2\ln 2}\sum_{l=0}^{c}\binom{c}{l}\beta^{c-l}\sum_{i=1}^{I_1}\rho_i\left(\frac{\bar{\gamma}_{3,i}^{d-l}}{\bar{\gamma}_1^{d-l}\Gamma\left(d\right)}I_{A,3}+\frac{\varepsilon\delta\bar{\gamma}_{3,i}^{d-l+1}}{\Gamma\left(d+1\right)}I_{A,4}\right), \tag{A.8}$$

where

$$I_{A,3}=\int_0^\infty x^{d-l-1}\mathrm{G}_{2,2}^{1,2}\left[x\middle|\begin{matrix}1,1\\1,0\end{matrix}\right]\mathrm{G}_{2,2}^{1,2}\left[\frac{\left(\beta-\delta\right)\bar{\gamma}_{3,i}x}{\bar{\gamma}_1}\middle|\begin{matrix}-d+l,1-d\\0,1-d+l\end{matrix}\right]dx, \tag{A.9}$$

$$I_{A,4}=\int_0^\infty x^{d-l}\mathrm{G}_{2,2}^{1,2}\left[x\middle|\begin{matrix}1,1\\1,0\end{matrix}\right]\mathrm{G}_{2,2}^{1,2}\left[\frac{\left(\beta-\delta\right)\bar{\gamma}_{3,i}x}{\bar{\gamma}_1}\middle|\begin{matrix}-d+l-1,-d\\0,-d+l\end{matrix}\right]dx, \tag{A.10}$$

By utilizing the integration relationship [33, eq. (21)], $I_{A,3}$ and $I_{A,4}$ can be computed as

$$I_{A,3}=\mathrm{G}_{4,4}^{3,3}\left[\eta\middle|\begin{matrix}-d+l,1-d,-d+l,1-d+l\\0,-d+l,-d+l,1-d+l\end{matrix}\right], \tag{A.11}$$

$$I_{A,4}=\mathrm{G}_{4,4}^{3,3}\left[\eta\middle|\begin{matrix}-d+l-1,-d,-d+l-1,-d+l\\0,-d+l-1,-d+l-1,-d+l\end{matrix}\right]. \tag{A.12}$$

To this end, by substituting (A.11) and (A.12) into (A.8) along with some mathematical computations, the desired result of C_1 is given by (18).

Similarly, by using (7), (11) into (17) and [26, eq. (3.351.3)], $f_{\Gamma_2}\left(x\right)$ can be obtained as

$$f_{\Gamma_2}\left(x\right)=\frac{x^{N_d-1}}{\left(N_d-1\right)!\bar{\gamma}_2^{N_d}}\sum_{j=1}^{I_2}\frac{\omega_j N_d!}{\bar{\gamma}_{4,j}}\left(\frac{x}{\bar{\gamma}_2}+\frac{1}{\bar{\gamma}_{4,j}}\right)^{-N_d-1}. \tag{A.13}$$

Then, substituting (A.13) into (15) along with (A.9) yields

$$C_2=\frac{1}{2\ln 2\left(N_d-1\right)!\bar{\gamma}_2^{N_d}}\sum_{j=1}^{I_2}\omega_j N_d!\bar{\gamma}_{4,j}^{N_d}\underbrace{\int_0^\infty x^{N_d-1}\left(1+\frac{\bar{\gamma}_{4,j}x}{\bar{\gamma}_2}\right)^{-N_d-1}\mathrm{G}_{1,1}^{1,1}\left[\frac{\bar{\gamma}_{4,j}}{\bar{\gamma}_2}x\middle|\begin{matrix}-N_d\\0\end{matrix}\right]dx}_{I_{A,5}}. \tag{A.14}$$

To solve the integral, we first express $\left(1+\bar{\gamma}_{4,j}x/\bar{\gamma}_2\right)^{-N_d-1}$ in terms of Meijer-G function as [33,

eq. (10)]

$$\left(1+\frac{\bar{\gamma}_{4,j}x}{\bar{\gamma}_2}\right)^{-N_d-1}=\frac{1}{\Gamma\left(N_d+1\right)}\mathrm{G}_{1,1}^{1,1}\left[\frac{\bar{\gamma}_{4,j}}{\bar{\gamma}_2}x\,\middle|\,\begin{matrix}-N_d\\0\end{matrix}\right]. \tag{A.15}$$

Then, using [33, eq. (21)], we can further obtain

$$I_{A,5}=\frac{1}{\Gamma\left(N_d+1\right)}\mathrm{G}_{3,3}^{3,2}\left[\frac{\bar{\gamma}_{4,j}}{\bar{\gamma}_2}\,\middle|\,\begin{matrix}-N_d,-N_d,-N_d+1\\0,-N_d,-N_d\end{matrix}\right]. \tag{A.16}$$

Finally, by substituting (A.16) into (A.14), the analytical expression of C_2 can be given by (19).

APPENDIX B
PROOF OF THEOREM 2

By substituting (A.6) and (A.13) into (21) and applying [26, eq. (7.813.1)], the MGF of Γ_1 and Γ_2 can be, respectively, obtained as

$$M_{\Gamma_1}\left(s\right)=\alpha^{N_s}\sum_{l=0}^{c}\left(\begin{matrix}c\\l\end{matrix}\right)\beta^{c-l}\sum_{i=1}^{I_1}\rho_i\left(\frac{\bar{\gamma}_{3,i}^{d-l}}{\Gamma\left(d\right)\bar{\gamma}_1^{d-l}}\varphi_1+\frac{\varepsilon\delta\bar{\gamma}_{3,i}^{d-l+1}}{\Gamma\left(d+1\right)\bar{\gamma}_1^{d-l+1}}\varphi_2\right), \tag{B.1}$$

and

$$M_{\Gamma_2}\left(s\right)=\frac{1}{(N_d-1)!\bar{\gamma}_2^{N_d}}\sum_{j=1}^{I_2}\varphi_j\bar{\gamma}_{4,j}^{N_d}\varphi_3, \tag{B.2}$$

where

$$\varphi_1=s^{-d+l}\mathrm{G}_{3,2}^{1,3}\left[\frac{\left(\beta-\delta\right)\bar{\gamma}_{3,i}}{\bar{\gamma}_1 s}\,\middle|\,\begin{matrix}-d+l+1,-d+l,1-d\\0,1-d+l\end{matrix}\right], \tag{B.3}$$

$$\varphi_2=s^{-d+l+1}\mathrm{G}_{3,2}^{1,3}\left[\frac{\left(\beta-\delta\right)\bar{\gamma}_{3,i}}{\bar{\gamma}_1 s}\,\middle|\,\begin{matrix}-d+l,-d+l-1,-d\\0,-d+l\end{matrix}\right], \tag{B.4}$$

$$\varphi_3=s^{-N_d}\mathrm{G}_{2,1}^{1,2}\left[\frac{\bar{\gamma}_{4,j}}{\bar{\gamma}_2 s}\,\middle|\,\begin{matrix}-N_d+1,-N_d\\0\end{matrix}\right]. \tag{B.5}$$

According to the well-known derivative property of $\left[f_1\left(x\right)f_2\left(x\right)\right]^{(1)}=f_1^{(1)}\left(x\right)f_2\left(x\right)+f_1\left(x\right)f_2^{(1)}\left(x\right)$, where $f_i^{(1)}\left(x\right)$ denotes the first-order derivative of $f_i\left(x\right)$ with respect to x, $M_{\Gamma_3}^{(1)}\left(s\right)$ can be expressed as

$$M_{\Gamma_3}^{(1)}\left(s\right)=M_{\Gamma_1}^{(1)}\left(s\right)M_{\Gamma_2}\left(s\right)+M_{\Gamma_1}\left(s\right)M_{\Gamma_2}^{(1)}\left(s\right), \tag{B.6}$$

Now, we turn to derive the expressions of $M_{\Gamma_i}^{(1)}\,(i=1,2)$. By using the following identity [39, eq. (8.2.2.14)]

$$\mathrm{G}_{p,q}^{m,n}\left[x^{-1}\left|\begin{array}{c}\mathbf{a}_p\\ \mathbf{b}_q\end{array}\right.\right]=\mathrm{G}_{q,p}^{n,m}\left[x\left|\begin{array}{c}1-\mathbf{b}_q\\ 1-\mathbf{a}_p\end{array}\right.\right], \tag{B.7}$$

$\varphi_i\,(i=1,2,3)$ can be first written as

$$\varphi_1=s^{-d+l}\mathrm{G}_{2,3}^{3,1}\left[\frac{\bar{\gamma}_1 s}{(\beta-\delta)\,\bar{\gamma}_{3,i}}\left|\begin{array}{c}1,d-l\\ d-l,d-l+1,d\end{array}\right.\right], \tag{B.8}$$

$$\varphi_2=s^{-d+l-1}\mathrm{G}_{2,3}^{3,1}\left[\frac{\bar{\gamma}_1 s}{(\beta-\delta)\,\bar{\gamma}_{3,i}}\left|\begin{array}{c}1,1+d-l\\ d-l+1,d-l+2,1+d\end{array}\right.\right], \tag{B.9}$$

$$\varphi_3=s^{-N_d}\mathrm{G}_{1,2}^{2,1}\left[\frac{\bar{\gamma}_2 s}{\bar{\gamma}_{4,j}}\left|\begin{array}{c}1\\ N_d,N_d+1\end{array}\right.\right]. \tag{B.10}$$

Then, from [39, eq. (8.2.2.38)],

$$\frac{d}{dz}\left[z^{-b_1}\mathrm{G}_{p,q}^{m,n}\left[z\left|\begin{array}{c}\mathbf{a}_p\\ \mathbf{b}_q\end{array}\right.\right]\right]=-\,z^{-1-b_1}\mathrm{G}_{p,q}^{m,n}\left[z\left|\begin{array}{c}\mathbf{a}_p\\ b_1+1,b_2,\cdots,b_q\end{array}\right.\right](m\geq 1), \tag{B.11}$$

we can obtain the further obtain $\varphi_i^{(1)}\,(i=1,2,3)$ as

$$\varphi_1^{(1)}=-s^{-d+l-1}\mathrm{G}_{2,3}^{3,1}\left[\frac{\bar{\gamma}_1 s}{(\beta-\delta)\,\bar{\gamma}_{3,i}}\left|\begin{array}{c}1,d-l\\ d-l+1,d-l+1,d\end{array}\right.\right], \tag{B.12}$$

$$\varphi_2^{(1)}=-s^{-d+l-2}G_{2,3}^{3,1}\left[\frac{\bar{\gamma}_1 s}{(\beta-\delta)\,\bar{\gamma}_{3,i}}\left|\begin{array}{c}1,1+d-l\\ d-l+2,d-l+2,1+d\end{array}\right.\right], \tag{B.13}$$

$$\varphi_3^{(1)}=-s^{-N_d-1}\mathrm{G}_{1,2}^{2,1}\left[\frac{\bar{\gamma}_2 s}{\bar{\gamma}_{4,j}}\left|\begin{array}{c}1\\ N_d+1,N_d+1\end{array}\right.\right]. \tag{B.14}$$

Thus, the analytical expression of $M_{\Gamma_i}^{(1)}\,(i=1,2)$ is given by

$$M_{\Gamma_1}^{(1)}(s)=\alpha^{N_s}\sum_{l=0}^{c}\binom{c}{l}\beta^{c-l}\sum_{i=1}^{I_1}\rho_i\left(\frac{\bar{\gamma}_{3,i}^{d-l}}{\Gamma(d)\,\bar{\gamma}_1^{d-l}}\varphi_1^{(1)}+\frac{\varepsilon\delta\bar{\gamma}_{3,i}^{d-l+1}}{\Gamma(d+1)\,\bar{\gamma}_1^{d-l+1}}\varphi_2^{(1)}\right), \tag{B.15}$$

$$M_{\Gamma_2}^{(1)}(s)=\frac{1}{(N_d-1)!\bar{\gamma}_2^{N_d}}\sum_{j=1}^{I_2}\varphi_j\bar{\gamma}_{4,j}^{N_d}\varphi_3^{(1)}. \tag{B.16}$$

By substituting (B.1), (B.2), (B.15) and (B.16) into (B.6), one can obtain

$$M_{\Gamma_3}^{(1)}(s)=\alpha^{N_s}\sum_{l=0}^{c}\binom{c}{l}\beta^{c-l}\sum_{i=1}^{I_1}\rho_i\sum_{j=1}^{I_2}\frac{\varphi_j\bar{\gamma}_{4,j}^{N_d}}{(N_d-1)!\bar{\gamma}_2^{N_d}}\varphi_3\left(\frac{\bar{\gamma}_{3,i}^{d-l}}{\Gamma(d)\,\bar{\gamma}_1^{d-l}}\varphi_1^{(1)}+\frac{\varepsilon\delta\bar{\gamma}_{3,i}^{d-l+1}}{\Gamma(d+1)\,\bar{\gamma}_1^{d-l+1}}\varphi_2^{(1)}\right)$$
$$\alpha^{N_s}\sum_{l=0}^{c}\binom{c}{l}\beta^{c-l}\sum_{i=1}^{I_1}\rho_i\sum_{j=1}^{I_2}\frac{\varphi_j\bar{\varphi}_{4,j}^{N_d}}{(N_d-1)!\bar{\gamma}_2^{N_d}}\varphi_3^{(1)}\left(\frac{\bar{\gamma}_{3,i}^{d-l}}{\Gamma(d)\,\bar{\gamma}_1^{d-l}}\varphi_1+\frac{\varepsilon\delta\bar{\gamma}_{3,i}^{d-l+1}}{\Gamma(d+1)\,\bar{\gamma}_1^{d-l+1}}\varphi_2\right). \quad \text{(B.17)}$$

Finally, from (20) and (B.17), the closed-form expression for C_3 is given by

$$C_3=\frac{\alpha^{N_s}}{\ln 2}\sum_{l=0}^{c}\binom{c}{l}\beta^{c-l}\sum_{i=1}^{I_1}\rho_i\sum_{j=1}^{I_2}\frac{\varphi_j\bar{\gamma}_{4,j}^{N_d}}{(N_d-1)!\bar{\gamma}_2^{N_d}}$$
$$\times\left(\frac{\bar{\gamma}_{3,i}^{d-l}}{\Gamma(d)\,\bar{\gamma}_1^{d-l}}\left[\int_0^{\infty}Ei(-x)\,\varphi_1^{(1)}\varphi_3dx+\int_0^{\infty}Ei(-x)\,\varphi_1\varphi_3^{(1)}dx\right]\right.$$
$$\left.+\frac{\varepsilon\delta\bar{\gamma}_{3,i}^{d-l+1}}{\Gamma(d+1)\,\bar{\gamma}_1^{d-l+1}}\left[\int_0^{\infty}Ei(-x)\,\varphi_2^{(1)}\varphi_3dx+\int_0^{\infty}Ei(-x)\,\varphi_2\varphi_3^{(1)}dx\right]\right). \quad \text{(B.18)}$$

To solve the four integrals in (B.18), we first apply the identity [39, eq. (8.4.11.1)] to express the $Ei(-s)$ in terms of Meijer-G function as

$$Ei(-s)=-G_{1,2}^{2,0}\left[s\left|\begin{matrix}1\\0,0\end{matrix}\right.\right]. \quad \text{(B.19)}$$

With the aid of the [27, eq. (3.1)], the closed-form expression for C_3 can be expressed as (22).

REFERENCES

[1] A. Vanelli-Coralli, G. Corazza, G. Karagiannidis, P. Mathiopoulos, D. Michalopoulos, C. Mosquera, S. Papaharalabos, and S. Scalise, "Satellite communications: Research trends and open issues," in *Proc. of the International Workshop on Satellite and Space Communications, IWSSC'07.*, Siena-Tuscany Italy, Sep. 2007, pp. 71-75.

[2] J. N. Laneman, D. N. C. Tse, and G. W. Wornell, "Cooperative diversity in wireless networks: efficient protocols and outage behavior," *IEEE Trans. Inf. Theory*, vol. 50, no. 12, pp. 3062-3080, Dec. 2004.

[3] B. Evans, M. Werner, E. Lutz, M. Bousquet, G. Corazza, G. Maral and R. Rumeau, "Integration of satellite and terrestrial systems in future media communications," *IEEE Trans. Wireless Commun.*, vol. 12, no. 5, pp. 72-80, Oct. 2005.

[4] M. R. Bhatnagar and M. K. Arti, "Performance analysis of AF based hybrid satellite-terrestrial cooperative network over generalize fading channels," *IEEE Commun. Lett.*, vol. 17, no. 10, pp. 1912-1915, Oct. 2013.

[5] M. R. Bhatnagar and Arti M.K., "Performance analysis of hybrid satellite-terrestrial FSO cooperative system," *IEEE Photonics Technol. Lett.*, vol. 25, no. 22, pp. 2197-2200, Nov. 2013.

[6] S. Sreng, B. Escrig and M.-L. Boucheret, "Exact outage probability of a hybrid satellite terrestrial cooperative system with best Relay selection," in *Proc. of IEEE ICC 2013*, Budapest, Hungary, June 2013, pp. 4520-4524.

[7] K. P. Liolis, A. D. Panagopoulos, and P. G. Cottis, "Multi-satellite MIMO communications at Ku-band and above: Investigations on spatial multiplexing for capacity improvement and selection diversity for interference mitigation," *EURASIP J. Wireless Commun. Netw.*, no. 2, July 2007.

[8] V. K. Sakarellos and A. D. Panagopoulos, "Outage performance of cooperative land mobile satellite broadcasting systems, in *Proc. 2013 European Conference on Antennas and Propagation*, Gothenburg, Sweden, Apr. 2013, 473-476.

[9] V. K. Sakarellos, C. Kourogiorgas and A. D. Panagopoulos, "Cooperative hybrid land mobile satellite-terrestrial broadcasting systems: outage probability evaluation and accurate simulation", *Wireless Personal Commun.*, vol. 79, no. 2, pp. 1471-1481, Nov. 2014.

[10] R. H. Y. Louie, Y. Li, H. A. Suraweera, and B. Vucetic, "Performance analysis of beamforming in two hop amplify and forward relay networks with antenna correlation," *IEEE Trans. Wireless Commun.*, vol. 8, no. 6, pp. 3132-3141, June 2009.

[11] M. Li, M. Lin, and Q. Yu, W.-P. Zhu and Lei Dong, "Optimal beamformer design for two hop MIMO AF relay networks over Rayleigh fading channels," *IEEE J. Sel. Areas Commun.*, vol. 30, no. 8, pp. 1402-1414, Sep. 2012.

[12] P. Arapoglou, K. Liolis, M. Bertinelli, A. Panagopoulos, and *etal*, "MIMO over satellite: A review," *IEEE Commun. Surveys Tut.*, vol. 13, no. 1, pp. 27-51, May 2011.

[13] G. Alfano and A. D. Maio, "Sum of squared Shadowed-Rice random variables and its application to communication systems performance prediction, *IEEE Trans. Wireless Commun.*, vol. 6, no. 10, pp. 3540-3545, Oct. 2007.

[14] Arti M.K., "Imperfect CSI Based Maximal Ratio Combining in Shadowed-Rician Fading Land Mobile Satellite Channels," *National Conference on Communications (NCC)*, Mumbai, India, Feb-March 2015.

[15] Y. Dhungana and N. Rajatheva, "Analysis of LMS based dual hop MIMO systems with beamforming," in *Proc. of IEEE ICC 2011*, Kyoto, Janpan, June 2011, pp. 1-6.

[16] Arti M.K. and M. R. Bhatnagar, "Beamforming and combining in hybrid satellite-terrestrial cooperative systems," *IEEE Commun. Lett.*, vol. 18, no. 3, pp. 483-486, Mar. 2014.

[17] M. R. Bhatnagar, "Performance evaluation of decode-and-forward satellite relaying," *IEEE Trans. Veh. Technol., accepted for publication*, in 2015.

[18] N. I. Miridakis, D. D. Vergados, and A. Michalas, "Dual-hop Communication over a Satellite Relay and Shadowed Rician Channels," *IEEE Trans. Veh. Technol., accepted for publication*, in 2015.

[19] Arti M.K. and M. R. Bhatnagar, "Two-way mobile satellite relaying: A beamforming and combining based approach," *IEEE Commun. Lett.*, vol. 18, no. 7, pp. 1187-1190, July 2014.

[20] Y. Dhungana, N. Rajatheva and C. Tellambura, "Performance Analysis of Antenna Correlation on LMS-Based Dual-Hop AF MIMO Systems," *IEEE Trans. Veh. Technol.*, vol. 61, no. 8, pp. 3590-3602, Oct. 2012.

[21] H. A. Suraweera, H. K. Garg and A. Nallanathan, "Performance analysis of two hop amplify-and-forward systems with interference at the relay," *IEEE Commun. Lett.*, vol. 14, no. 8, pp. 692-694, Aug. 2010.

[22] C. Zhong, S. Jin, and K. K. Wong, "Dual-hop systems with noisy relay and interference-limited destination," *IEEE Trans. Commun.*, vol. 58, no. 3, pp. 764-768, Mar. 2010.

[23] C. Zhong, H. Suraweera, A. Huang, Z. Zhang, and C. Yuen, "Outage probability of dual-hop multiple antenna AF relaying systems with interference," *IEEE Trans. Commun.*, vol. 61, no. 1, pp. 108-119, Jan. 2013.

[24] M. Sadek and S. Aissa, "Personal satellite communication: technologies and challenges", *IEEE Wireless Commun.*, vol. 12, no. 5, pp. 28-35, Dec. 2012.

[25] K. An, M. Lin, J. Ouyang, Y. Huang and G. Zheng, "Symbol error analysis of hybrid satellite-terrestrial cooperative networks with co-channel interference" *IEEE Commun. Lett.*, vol. 18, no. 11, pp. 1947-1950, Nov. 2014.

[26] I. S. Gradshteyn and I. M. Ryzhik, *Table of Integrals, Series, and Products, 7th ed.* Academic Press, 2007.

[27] R. P. Agrawal, "Certain transformation formulae and Meijer's G function of two variables," *Indian J. Pure Appl. Math.*, vol. 1, no. 4, 1970.

[28] A. Abdi,W. Lau, M.-S. Alouini, and M. Kaveh, "A new simple model for land mobile satellite channels: first- and second-order statistics," *IEEE Trans. Wireless Commun.*, vol. 2, no. 3, pp. 519-528, May 2003.

[29] M. R. Bhatnagar and Arti M.K., "On the closed-form performance analysis of maximal ratio combining in Shadowed-Rician fading LMS channels," *IEEE Commun. Lett.*, vol. 18, no. 1, pp. 54-57, Jan. 2014.

[30] M. Di Renzo, F. Graziosi, and F. Santucci, "Channel capacity over generalized fading channels: a novel MGF-based approach for performance analysis and design of wireless communication systems," *IEEE Trans. Veh. Technol.*, vol. 59, no. 1, pp. 127-149, Jan. 2010.

[31] I. S. Ansari, F. Yilmaz, and M.-S. Alouini, "Performance analysis of FSO links over unified Gamma-Gamma turbulence channels," in *Proc. of IEEE Vehicular Technology Conference (VTC Spring 2015)*, Glasgow, Scotland, May 2015, pp. 1-5.

[32] I. S. Ansari, S. Al-Ahmadi, F. Yilmaz, M.-S. Alouini and H. Yanikomeroglu, "A new formula for the BER of binary modulations with dual-branch selection over generalized-K composite fading channels," *IEEE Trans. Commun.*, vol. 59, no. 10, pp. 2654-2658, Oct. 2011.

[33] V. S. Adamchik and O. I. Marichev, "The algorithm for calculating integrals of hypergeometric type functions and its realization in reduce systems," in *Proc. Int. Conf. Symp. Algebraic Comput.*, 1990, pp. 212-224.

[34] M. K. Simon and M. S. Alouini, *Digital Communications over Fading Channels: A Unified Approach to Performance Analysis*. Wiley, 2000.

[35] M. Chiani, D. Dardari, and M. K. Simon, "New exponential bounds and approximations for the computation of error probability in fading channels," *IEEE Trans. Wireless Commun.*, vol. 2, no. 4, pp. 840-845, July 2003.

[36] J. G. Proakis, *Digital Communications*, 4th ed. New York: McGraw-Hill, 2001.

[37] K. Roach, "Meijer-G function representations," in Proc. ACM International Conf. Symbolic Algebraic Computation, pp. 205-211, July 1997.

[38] M. Abramowitz, I. A. Stegun, *Handbook of mathematical functions with formulas, graphs, and mathematical tables*, 10th ed. New York: Dover publications, 1972.

[39] A. P. Prudnikov, Y. A. Brychkov, and O. I. Marichev, *Integrals and Series*, 1st ed. Gordon and Breach Science Publishers, 1990, vol. 3.